Published in final edited form as:
Proc SPIE. 2013 March 14; 8671: . doi:10.1117/12.2007695.

Accuracy Evaluation of a 3D Ultrasound-guided Biopsy System

Walter J. Wooten III[a], **Jonathan A. Nye**[a], **David M. Schuster**[a], **Peter T. Nieh**[b], **Viraj A. Master**[b], **John R. Votaw**[a], and **Baowei Fei**[a,c,d,*]

[a]Department of Radiology and Imaging Sciences, Emory University, Atlanta, GA

[b]Department of Urology, Emory University School of Medicine, Atlanta, GA

[c]Department of Biomedical Engineering, Emory University and Georgia Institute of Technology

[d]Department of Mathematics and Computer Science, Emory University, Atlanta, GA

Abstract

Early detection of prostate cancer is critical in maximizing the probability of successful treatment. Current systematic biopsy approach takes 12 or more randomly distributed core tissue samples within the prostate and can have a high potential, especially with early disease, for a false negative diagnosis. The purpose of this study is to determine the accuracy of a 3D ultrasound-guided biopsy system. Testing was conducted on prostate phantoms created from an agar mixture which had embedded markers. The phantoms were scanned and the 3D ultrasound system was used to direct the biopsy. Each phantom was analyzed with a CT scan to obtain needle deflection measurements. The deflection experienced throughout the biopsy process was dependent on the depth of the biopsy target. The results for markers at a depth of less than 20 mm, 20-30 mm, and greater than 30 mm were 3.3 mm, 4.7 mm, and 6.2 mm, respectively. This measurement encapsulates the entire biopsy process, from the scanning of the phantom to the firing of the biopsy needle. Increased depth of the biopsy target caused a greater deflection from the intended path in most cases which was due to an angular incidence of the biopsy needle. Although some deflection was present, this system exhibits a clear advantage in the targeted biopsy of prostate cancer and has the potential to reduce the number of false negative biopsies for large lesions.

Keywords

Prostate biopsy; transrectal ultrasound; phantom; ultrasound-guided; targeted biopsy; prostate cancer; 3D ultrasound imaging

1. INTRODUCTION

One in six men will be diagnosed with cancer of the prostate during their lifetime [1]. Systematic transrectal ultrasound (TRUS)-guided prostate biopsy is considered the standard method for prostate cancer diagnosis. The current two dimensional (2D) TRUS-guided biopsy technique has a significant sampling error and a low sensitivity (27%-40.3%) [2] and can miss up to 30% of cancers [3]. As a result, a patient may have a “negative” biopsy but may, in fact, be harboring an occult cancer. Alternatively, a diagnosis of cancer may have been made, but the patient is under-staged because the most aggressive histologic region of the tumor has not been sampled. Because of these limitations, patient management may not be optimized.

*Corresponding author: baowei.fei@emory.edu Website: www.feilab.org.

A 2D ultrasound image represents a thin plane in the body, yet the anatomy is three dimensions (3D), hence the physician must integrate multiple images in his/her mind. This practice is inefficient during interventional guidance, and may lead to variability and incorrect localization of lesions. Because of manually controlled scanning, it is difficult to localize the same image plane and reproduce it at a later time for follow-up studies. When using 2D transrectal ultrasound for needle-guidance, physicians have restricted anatomical reference points for guiding the needle to target sites. Any motion of the probe during the procedure may cause the prostate image to change or deform to a prohibitive extent. These variations make it difficult to establish a consistent frame of reference for needle guidance.

On the contrary, 3D ultrasound imaging provides volumetric representation of an object and offers images along any cross sections. The intuitive presentation by 3D ultrasound allows more accurate lesion localization and treatment planning [4] A 3D TRUS-guided system can record and display the 3D locations of biopsy cores [5-12], which is not possible with a conventional 2D image-guided system.

The purpose of this study was to determine the accuracy of a 3D ultrasound-guided biopsy system in prostate phantoms. Validation experiments were performed to determine the accuracy of the biopsy method with a visible target. The focus of this study was to determine the magnitude of the error inherent throughout the entirety of the biopsy process, from the initial scan to the firing of the biopsy needle. This includes image acquisition, planning, and needle guidance during the biopsy procedures. Prior knowledge of the accuracy of the overall system is necessary in order to successfully implement the biopsy technique in patient care.

2. METHODOLOGY

In this study, prostate phantoms with embedded markers were designed, scanned and biopsied using a 3D ultrasound guided biopsy system. The phantoms were created using an agar mixture which was combined with tungsten powder in the prostate portion of the phantom, and with cellulose in the background mixture. This mixture was optimized to allow adequate contrast on both ultrasound and CT images. Each prostate phantom had several markers of different material types embedded during the manufacturing process. Phantoms were crafted with softgel capsules containing vitamin A. Each phantom was scanned and biopsied using a 3D ultrasound navigation device (Artemis, Eigen Inc., Grass Valley, CA). After the biopsy process, CT images of each phantom were acquired to provide independent verification of the error analysis within the system.

2.1 Prostate phantom design

The design of the phantom was to create a prostate replica which would be visible to ultrasound and CT imaging modalities. Concentrations of the phantom mixtures were altered to produce variation in the acoustic impedance, which provided adequate contrast for ultrasound imaging. The background mixture contained cellulose scatter and the prostate portion of the phantom contained tungsten powder, which increased contrast for CT imaging. Actual creation of the phantom was initiated by the formation of the prostate which was obtained by pouring the prostate mixture into a negative mold of a prostate. The prostate portion was then placed in the refrigerator until solidification. After solidification, the background mixture was created, and poured around the prostate phantom in an acrylic phantom box. The phantom was refrigerated until solidification, and was then scanned and biopsied. A total of 13 prostate phantoms were created and used for this validation study.

2.2 System description

Imaging of the phantom was performed using a B&K ultrasound probe which was attached to the navigation device. Ultrasound gel was applied to the space between the probe and the phantom surface. The 3D ultrasound scan was completed by rotating the ultrasound probe while the navigation system captures the image series. This information was used to reconstruct a 3D representation of the prostate phantom, which shows the volume of the phantom, as well as the embedded markers. This information was then used to plan the biopsy and the biopsy sites were marked on the images. Each phantom contained four markers, allowing adequate space to accurately pair biopsy tracks with markers, as well as provided multiple depths and locations for the planned biopsy sites.

The actual biopsy was performed after the scanned prostate volume was segmented and after a target was assigned to the center of each visible marker. The center was determined by dividing the number of slices which contained the marker in half, and then using the visual center of the marker in the center slice. The navigation system used the assigned biopsy path to align the ultrasound probe for biopsy. The biopsy needle was inserted through a guidance sheath attached to the ultrasound probe and then was fired for core biopsy, which removed a cylindrical core from the phantom, leaving an air path which was visible in both ultrasound and CT imaging. The navigation system tracked the needle position during the biopsy process and measured the distance from the intended biopsy path to the air track created by the actual needle path. The deflection was recorded immediately after each biopsy.

2.3 CT validation

Although initial deflection distances were calculated from the acquired ultrasound data using the navigation system, independent verification of the deflection distance was necessary. CT analysis was chosen to perform this independent validation of the accuracy of the navigation system. After the completion of the biopsy process, each phantom received a CT scan which was used to measure the deflection of each air track from the respective target.

2.4 Data analysis

The software associated with the 3D ultrasound navigation system provided an internal error analysis for each biopsy procedure. This measured the deflection of the needle path as measured by the ultrasound guidance software in comparison to the intended path based on the target biopsy location selected within the prostate. This was conducted through internal mechanisms for the assessment of errors in the biopsy path, and required independent verification to ensure that a systematic error was not present in the determination of deflection from the intended path.

Error measurement was conducted within the system being tested, which called for outside verification of the deflection of the biopsy needle. A CT scan was performed on each of the phantoms biopsied to determine the distance from the air track to the center of the marker, as well as the depth of each marker from the surface of the phantom. To determine the deflection, the air track left by the needle path was identified and the distance from the center of the marker to the air track was recorded. Depth was determined by analyzing the coronal image of the phantoms and measuring the distance from the surface of the phantom to the marker.

3. RESULTS

The experiment was performed to determine the amount of the errors throughout the biopsy process from the initial ultrasound scan to the actual firing of the biopsy needle. Each embedded marker was used as a target for a biopsy, and the accuracy of the guidance system

was determined according to the proximity of the needle path compared to the intended path of the biopsy needle. The two primary variables measured throughout this experiment were the deflection of the biopsy needle and the depth of the marker being targeted. Table 1 shows the deflection of the biopsy needle for different depths, which illustrates the increase in errors associated with the increased depth of the marker in the phantom.

An average deflection of 3.3 mm was measured in the depths of less than 20 mm. Between 20 and 30 mm, the average deflection increased to 4.7 mm, and above 30 mm the deflection was 6.2 mm on average. The overall average deflection within the experiment ignoring depth was 4.9 mm over 51 trials. Figure 6 shows the correlation between the deflection and the depth of the biopsy path.

Statistical behavior of the ultrasound and CT data was examined using the t-test, which yielded a P-value of < 0.001, indicating that the accuracy measurements obtained from the ultrasound software were sufficient to determine the accuracy of the system.

4. DISCUSSION

Prostate phantoms were designed and tested using a 3D ultrasound guidance mechanism for targeted biopsy procedures. This study focused on the errors between the intended biopsy site and the actual needle track. This experiment provides comprehensive accuracy data for the entire biopsy process including all aspects of scanning, planning, and biopsy.

Three-dimensional ultrasound-guided biopsy has potential advantages over the traditional, 2D ultrasound-guided approach for prostate biopsy. By providing guidance to a specific lesion, targeted biopsy can be achieved by the biopsy process. In addition, 3D modeling of the actual needle path can provide a better representation of the specific location within the prostate which was biopsied, granting a higher degree of certainty as to whether the desired tissue sample was collected. This is especially beneficial when a suspicious area is being targeted, and allows for immediate re-biopsy in the event that the intended target was not successfully hit. Even without a clear target, a greater degree of knowledge of the biopsy path will be available for later analysis. This allows re-biopsy of a specific location in the event that tests were inconclusive, or avoidance of a clearly negative area of the prostate, favoring locations which were not previously biopsied for future testing.

The accuracy data is critical for clinical trials in human patients. Prior to implementation in a clinical setting, the performance characteristics of the guidance system must be thoroughly understood. By assessing the accuracy of the system in phantoms, sufficient information has been acquired to be able to determine the behavior of the system in a static environment. During imaging and interventional procedures of the prostate, other factors such as patient motion and prostate deformation can also contribute to the errors and various methods were proposed to tackled those problems [13-26].

Future applications of this technology would be to incorporate information from other imaging modalities into the planning phase of the biopsy process. This could possibly provide information allowing for the targeting of a specific location within the prostate for biopsy. Targeted biopsy would then have a much greater benefit in that suspicious lesions within the prostate could be targeted and accurately biopsies, granting a much higher level of confidence in the results of the test.

5. CONCLUSIONS

The primary factor affecting the deflection of the biopsy needle from the intended target was the depth of the marker. Increased depth caused increased error in the distance from the air

track to the marker. This finding seems to suggest that the size of the prostate being biopsied and the depth of the intended biopsy area will have an effect on the probability that the biopsy path will intersect with the intended target area of the biopsy. Reduction of the depth of the target and anticipation of possible deviation at greater depths will likely reduce the deflection of the biopsy needle from the intended path. Deflection was generally attributed to the angle of the biopsy needle being nonzero. Angular incidence of the biopsy needle resulted in a greater amount of deflection with increased depth. Despite the slight deflection, the system exhibits sufficient accuracy for targeted biopsy within a prostate phantom, and would prove useful in reducing the probability that a clinically significant tumor would not be detected. Incorporation of PET/CT or MR data would provide a target for the biopsy, which could be correlated with the 3D ultrasound image and implemented in the planning process for the biopsy procedure.

Acknowledgments

This research is supported in part by NIH grant R01CA156775 (PI: Fei), Georgia Cancer Coalition Distinguished Clinicians and Scientists Award (PI: Fei), and the Emory Molecular and Translational Imaging Center (NIH P50CA128301)

REFERENCES

1. Howlader, N.; Noone, AM.; Krapcho, M., et al. [SEER Cancer Statistics Review, 1975-2009 (Vintage 2009 Populations)]. National Cancer Institute; Bethesda, MD: 2012. http://seer.cancer.gov/csr/1975_2009_pops09
2. Pinto PA, Chung PH, Rastinehad AR, et al. Magnetic resonance imaging/ultrasound fusion guided prostate biopsy improves cancer detection following transrectal ultrasound biopsy and correlates with multiparametric magnetic resonance imaging. J Urol. 2011; 186(4):1281–5. [PubMed: 21849184]
3. Hricak H. MR imaging and MR spectroscopic imaging in the pre-treatment evaluation of prostate cancer. Br.J.Radiol. 2005; 78:S103–S111. [PubMed: 16306632]
4. Fenster A, Downey DB. Three-dimensional ultrasound imaging and its use in quantifying organ and pathology volumes. Anal Bioanal Chem. 2003; 377(6):982–9. [PubMed: 12955278]
5. Fei BW, Schuster DM, Master V, et al. A Molecular Image-directed, 3D Ultrasound-guided Biopsy System for the Prostate. Proc SPIE. 2012; 8316:831613. [PubMed: 22708023]
6. Fei BW, Master V, Nieh P, et al. A PET/CT directed, 3D ultrasound-guided biopsy system for prostate cancer. Workshop on Prostate Cancer Imaging at the Medical Imaging Computing and Image Assisted Interventions Meeting (MICCAI 2011) - Lecture Notes in Computer Science. 2011; 6963:100–108.
7. Akbari H, Fei BW. 3D ultrasound image segmentation using wavelet support vector machines. Medical Physics. 2012; 39:2972–2984. [PubMed: 22755682]
8. Yang X, Fei BW. 3D prostate segmentation of ultrasound images combining longitudinal image registration and machine learning. Proc SPIE. 2012; 8316:83162O.
9. Fei BW, Schuster DM, Master VA, et al. Incorporating PET/CT images into 3D ultrasound-guided biopsy of the prostate. Medical Physics. 2012; 39:3888.
10. Yang X, Schuster D, Master V, et al. Automatic 3D segmentation of ultrasound images using atlas registration and statistical texture prior. Proc SPIE. 2011; 7964:796432. [PubMed: 22708024]
11. Akbari H, Yang X, Halig LV, et al. 3D segmentation of prostate ultrasound images using wavelet transform. Proc SPIE. 2011; 7962:79622K.
12. Yang X, Akbari H, Halig L, et al. 3D non-rigid registration using surface and local salient features for transrectal ultrasound image-guided prostate biopsy. Proceedings of SPIE. 2011; 7964:79642V.
13. Fei BW, Duerk JL, Boll DT, et al. Slice-to-volume registration and its potential application to interventional MRI-guided radio-frequency thermal ablation of prostate cancer. IEEE Trans Med Imaging. 2003; 22(4):515–25. [PubMed: 12774897]

14. Fei BW, Duerk JL, Sodee DB, et al. Semiautomatic nonrigid registration for the prostate and pelvic MR volumes. Acad Radiol. 2005; 12(7):815–24. [PubMed: 16039535]
15. Fei BW, Duerk JL, Wilson DL. Automatic 3D registration for interventional MRI-guided treatment of prostate cancer. Comput Aided Surg. 2002; 7(5):257–67. [PubMed: 12582978]
16. Fei BW, Frinkley K, Wilson D, et al. Registration algorithms for interventional. MRI-guided treatment of the prostate. Proc SPIE. 2003; 5029:192–201.
17. Fei BW, Kemper C, Wilson D. Three-Dimensional Warping Registration of the Pelvis and Prostate. Proc. SPIE. 2002; 4684:528–537.
18. Fei BW, Kemper C, Wilson DL. A comparative study of warping and rigid body registration for the prostate and pelvic MR volumes. Comput Med Imaging Graph. 2003; 27(4):267–81. [PubMed: 12631511]
19. Fei BW, Lee Z, Boll D, et al. Image registration and fusion for interventional MRI guided thermal ablation of the prostate cancer. The Sixth Annual International Conference on Medical Imaging Computing & Computer Assisted Intervention. Lecture Notes in Computer Science (LNCS). 2003; 2879:364–372.
20. Fei BW, Lee Z, Duerk J, et al. Image registration for interventional MRI guided procedures: Interpolation methods, similarity measurements, and applications to the prostate. The Second International Workshop on Biomedical Image Registration - Lecture Notes in Computer Science (LNCS). 2003; 2717:321–329.
21. Fei BW, Wang H, Chen X, et al. In vivo small animal imaging for early assessment of therapeutic efficacy of photodynamic therapy for prostate cancer. Proceedings of SPIE. 2007; 6511:651102.
22. Fei BW, Wang H, Meyers JD, et al. High-field magnetic resonance imaging of the response of human prostate cancer to Pc 4-based photodynamic therapy in an animal model. Lasers Surg Med. 2007; 39(9):723–30. [PubMed: 17960753]
23. Fei BW, Wang H, Wu C, et al. Choline PET for monitoring early tumor response to photodynamic therapy. J Nucl Med. 2010; 51(1):130–8. [PubMed: 20008981]
24. Fei BW, Wheaton A, Lee Z, et al. Automatic MR volume registration and its evaluation for the pelvis and prostate. Phys Med Biol. 2002; 47(5):823–38. [PubMed: 11931473]
25. Fei BW, Wheaton A, Lee Z, et al. Robust registration method for interventional MRI-guided thermal ablation of prostate cancer. Proc. SPIE. 2001; 4319:53–60.
26. Fei BW, Wheaton A, Lee ZH, et al. Automatic MR volume registration and its evaluation for the pelvis and prostate. Physics in Medicine and Biology. 2002; 47(5):823–838. [PubMed: 11931473]

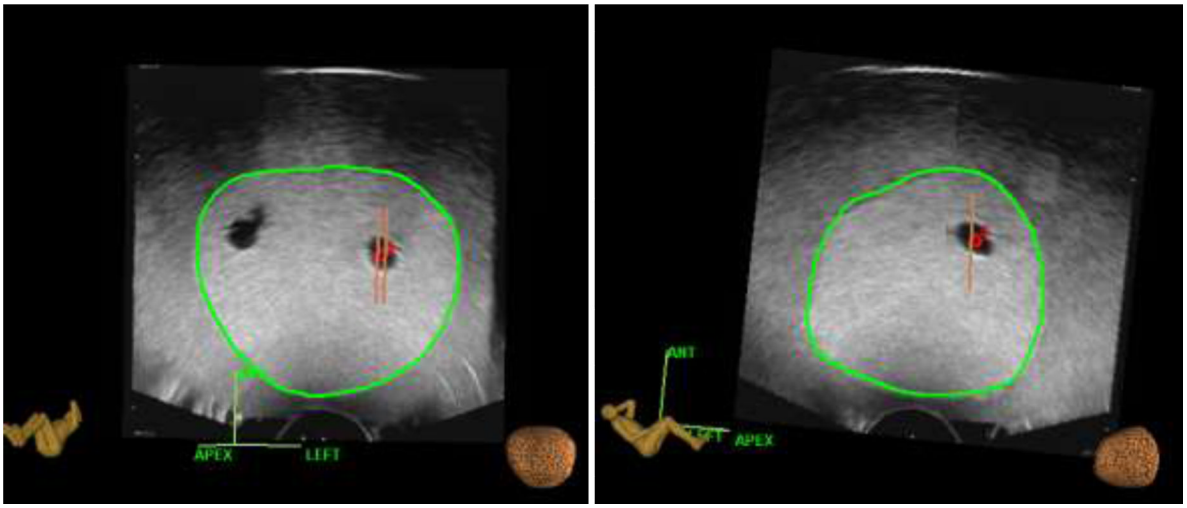

Figure 1.
Ultrasound scans of a prostate phantom in the biopsy planning phase. Prostate contouring has been completed and biopsy targets have been assigned to each marker.

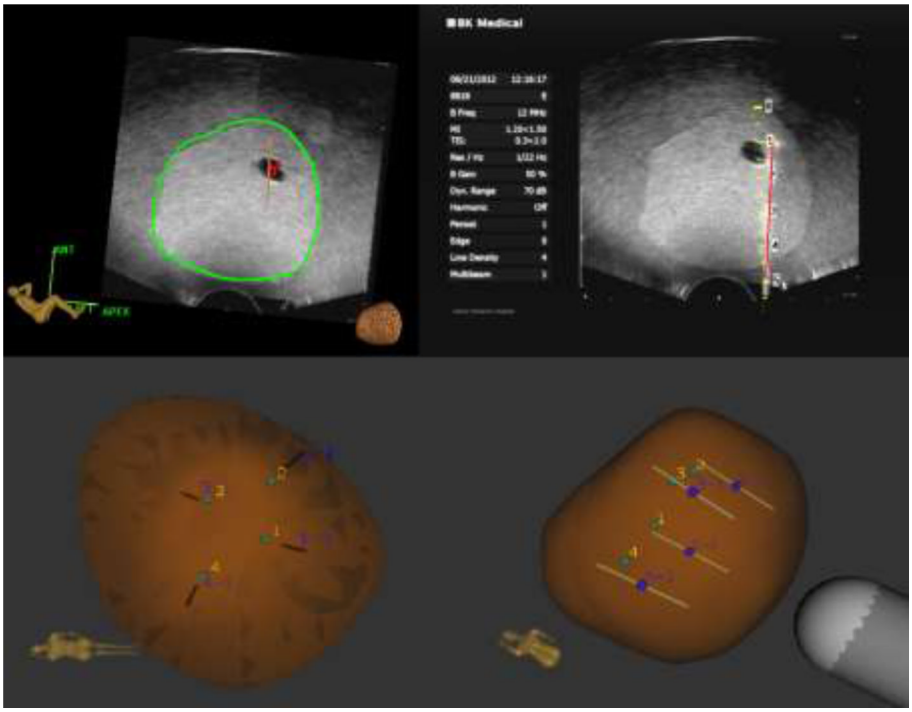

Figure 2.

Planning and biopsy images for Phantom 9. The upper left is the planning stage for Marker 1. The upper right is the actual biopsy being recorded for Marker 1. The bottom left is the transverse view of all planned sites with their respective actual biopsy paths. The bottom right is the lateral 3D view of each biopsy site in green while the blue dot is the center of the biopsy core. The biopsy core sample extends the length of the line passing through the actual biopsy site.

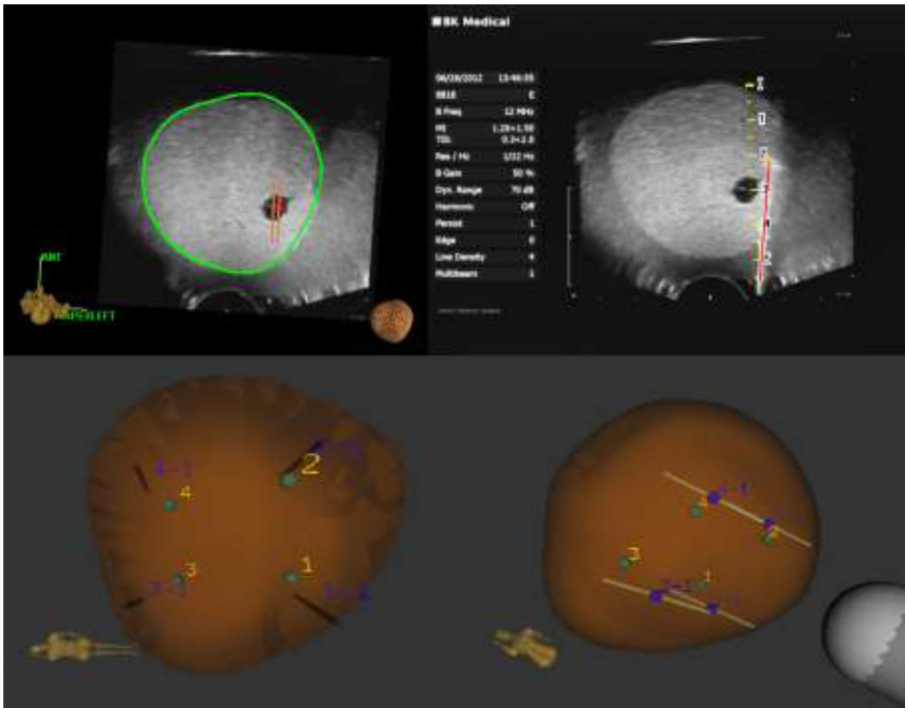

Figure 3.
Planning and biopsy images for Phantom 12. The bottom left is the transverse view of all planned sites with their respective actual biopsy paths. The bottom right is the lateral 3D view of each biopsy site in green while the blue dot is the center of the biopsy core. The biopsy core sample extends the length of the line passing through the actual biopsy site.

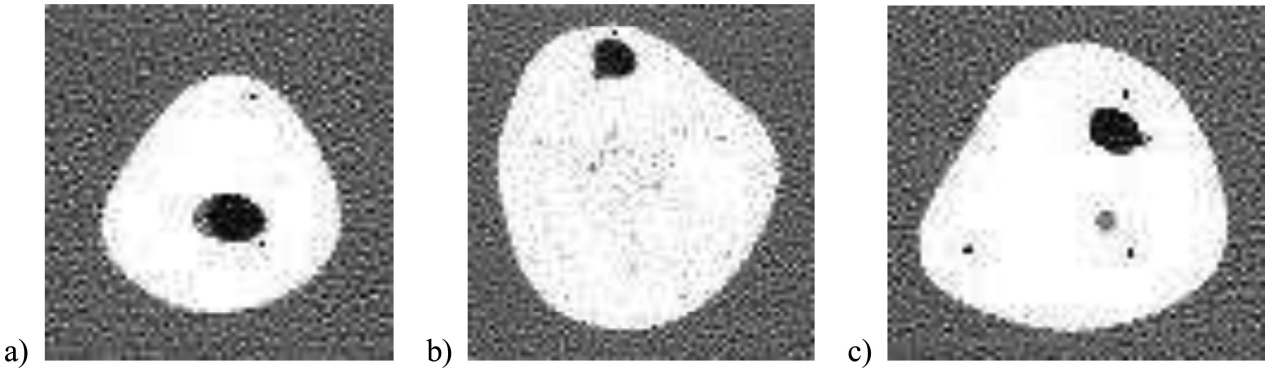

Figure 4.

CT images obtained from Phantoms 5 and 12. The needle tracks are clearly visible in these examples near the respective markers. Deflection was determined by measuring the distance from the needle track to the center of the marker. a) shows Marker 1 in Phantom 5; b) shows Marker 1 in Phantom 12; and c) shows Marker 2 in Phantom 12. The air tracks for other markers are also evident in this sample.

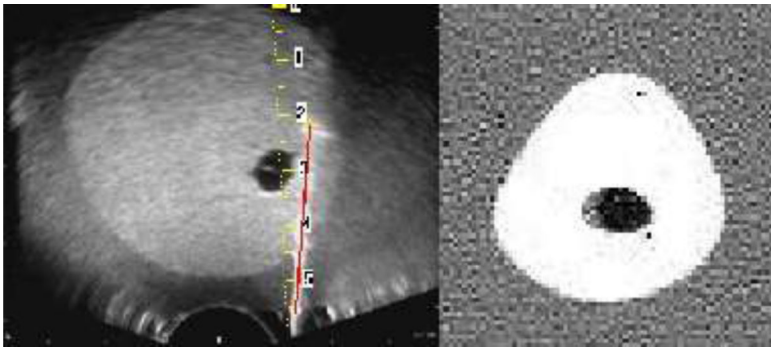

Figure 5.
Illustration of the correlation between the error measured by ultrasound and that measured by CT. The distance between the intended biopsy location and the needle path is internally measured by the ultrasound software. The CT images are used as the independent verification, and the distance between the air track left by the biopsy needle, and the center of the intended marker is measured to produce the accuracy results according to the CT data.

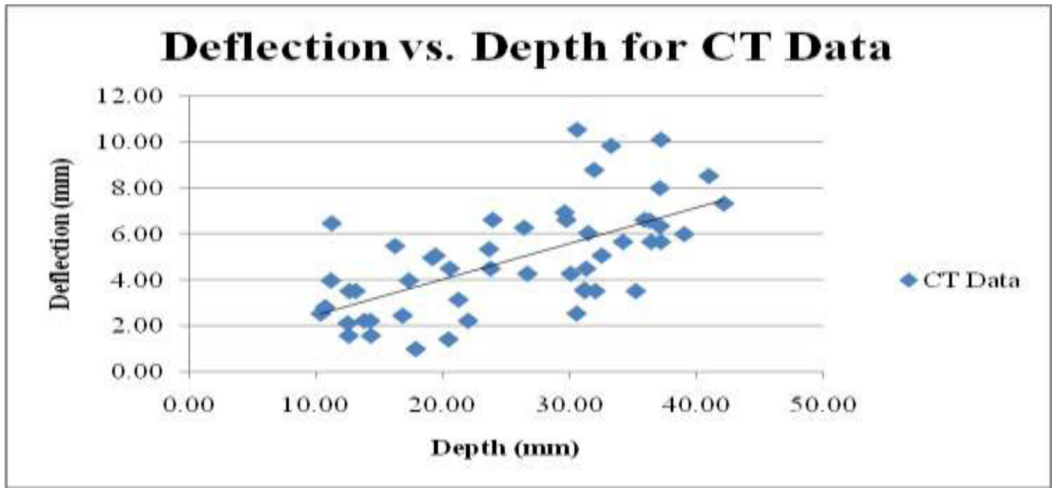

Figure 6.
Plot of the deflection of the biopsy path versus the depth of the intended target. Biopsy targets at greater depth tend to exhibit a higher amount of deflection than those targets at reduced depth.

Table 1

Deflection of the needle during biopsy of the prostate phantom at different depths. An increased depth generally caused an increase in the amount of deflection of the biopsy needle.

	Depth (mm)			
	< 20	**20-30**	**> 30**	**Total**
Number of Trials	17	11	23	51
Average Deflection	3.3	4.7	6.2	4.9
Standard Deviation	1.6	1.9	2.3	2.3

Table 2

Overall data of all trials combined which provides the angle of deflection for the biopsy needle.

	Deflection (mm)		Depth (mm)	Deflection Angle (degree)
	US	CT		
Mean	4.1	4.9	25.6	11.2
Median	3.7	4.5	17.3	10.3
Standard Deviation	1.9	2.3	9.5	4.7